Electronic Supplementary Information:

Mechanochemical Synthesis of Multi-Site Electrocatalysts as Bifunctional Zinc-Air Battery Electrodes

Beibei Guo,[a,b] Qiangjian Ju,[b,c] Ruguang Ma,[b,c] Zichuang Li,[b] Qian Liu,[b] Fei Ai,[b] Minghui Yang,*[c,d] Stefan Kaskel,[e] Jun Luo,[a] Tao Zhang,[b] and Jiacheng Wang*[b,c]

[a] School of Materials Science and Engineering, Shanghai University, Shanghai 200444, China

[b] State Key Laboratory of High Performance Ceramics and Superfine Microstructure, Shanghai Institute of Ceramics, Chinese Academy of Sciences, Shanghai 200050, China. Email: jiacheng.wang@mail.sic.ac.cn

[c] Center of Materials Science and Optoelectronics Engineering, University of Chinese Academy of Sciences, 100049 Beijing, China

[d] Ningbo Institute of Materials Technology and Engineering, Chinese Academy of Sciences, Ningbo 315201, China. Email: myang@nimte.ac.cn

[e] Department of Inorganic Chemistry, Dresden University of Technology, 01069 Dresden, Germany

Experimental

Chemicals.

Isophthalaldehyde, p-phenylenediamine, silica spheres and commercial RuO_2 were obtained from Aladdin Industrial Corporation. Cobaltous nitrate hexahydrate (II) ($Co(NO_3)_2 \cdot 6H_2O$) and ferric chloride ($FeCl_3$) were purchased from Sinopharm Chemical Reagent Co. Ltd. Nafion solution (5 wt%) were purchased from Aldrich. The commercial Pt/C catalyst (20 wt%) was obtained from Johnson Matthey (UK). All chemicals were utilized as received without any further purification.

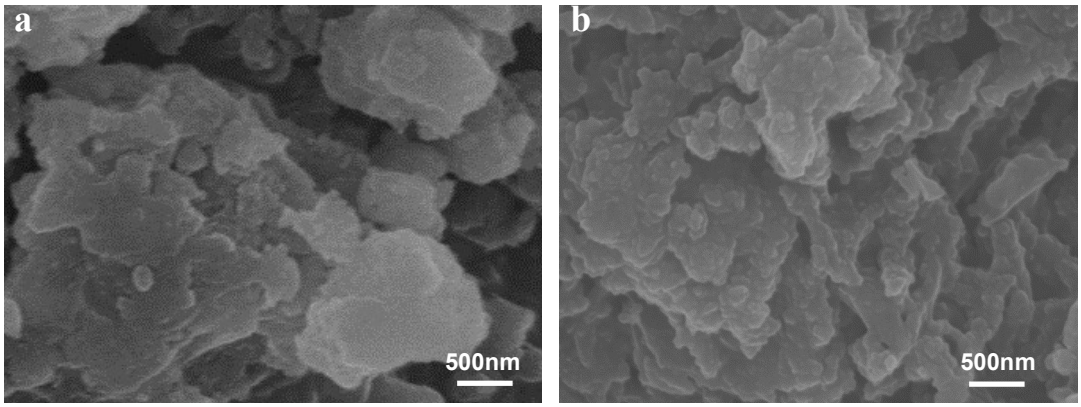

Fig. S1. SEM images of a) the polymer prepared by after ball milling, **b)** the pyrolyzed product.

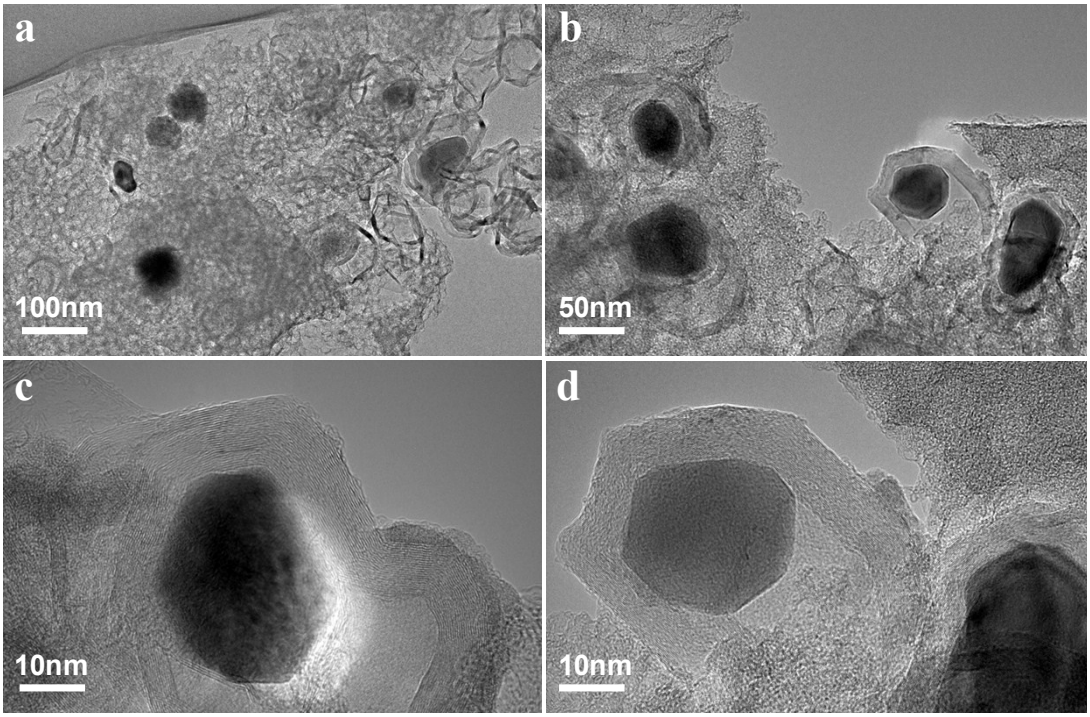

Fig. S2. TEM image of FeCo-NPC-1100.

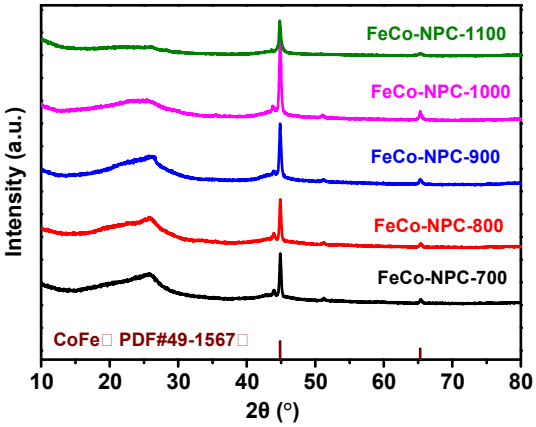

Fig. S3. XRD patterns of FeCo-NPC-700, FeCo-NPC-800, FeCo-NPC-900, FeCo-NPC-1000 and FeCo-NPC-1100.

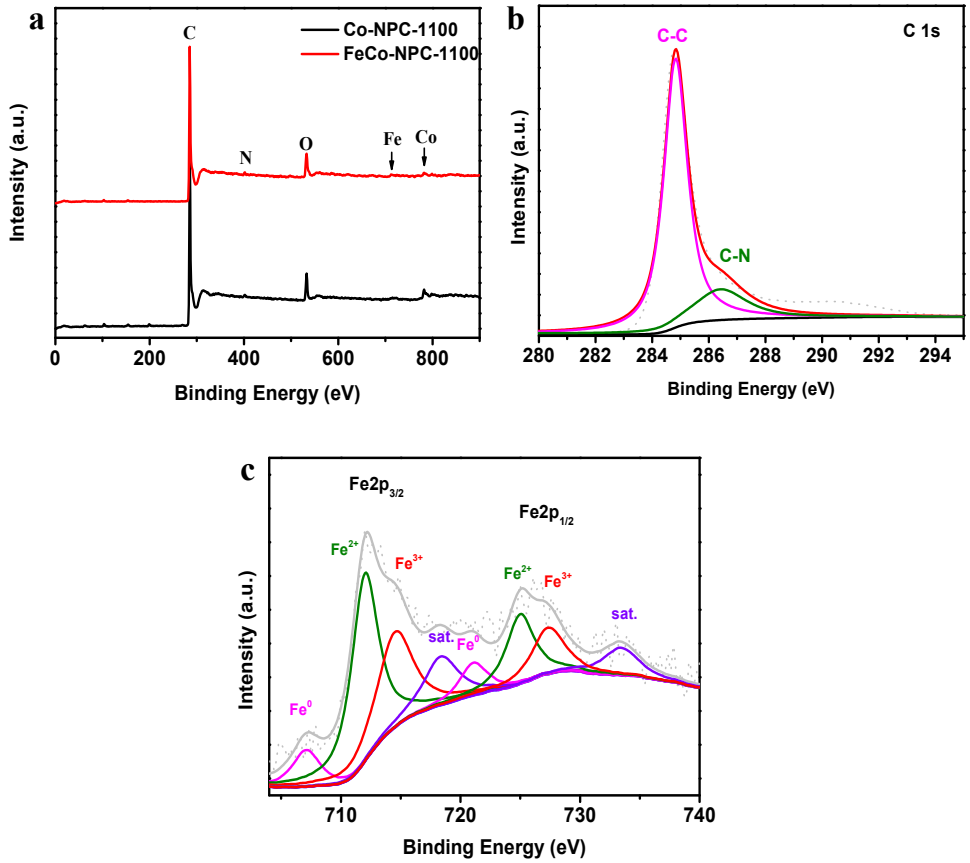

Fig. S4. a) XPS survey of Co-NPC-1100 and FeCo-NPC-1100; **b, c)** XPS spectra of C 1s and Fe2p for FeCo-NPC-1100.

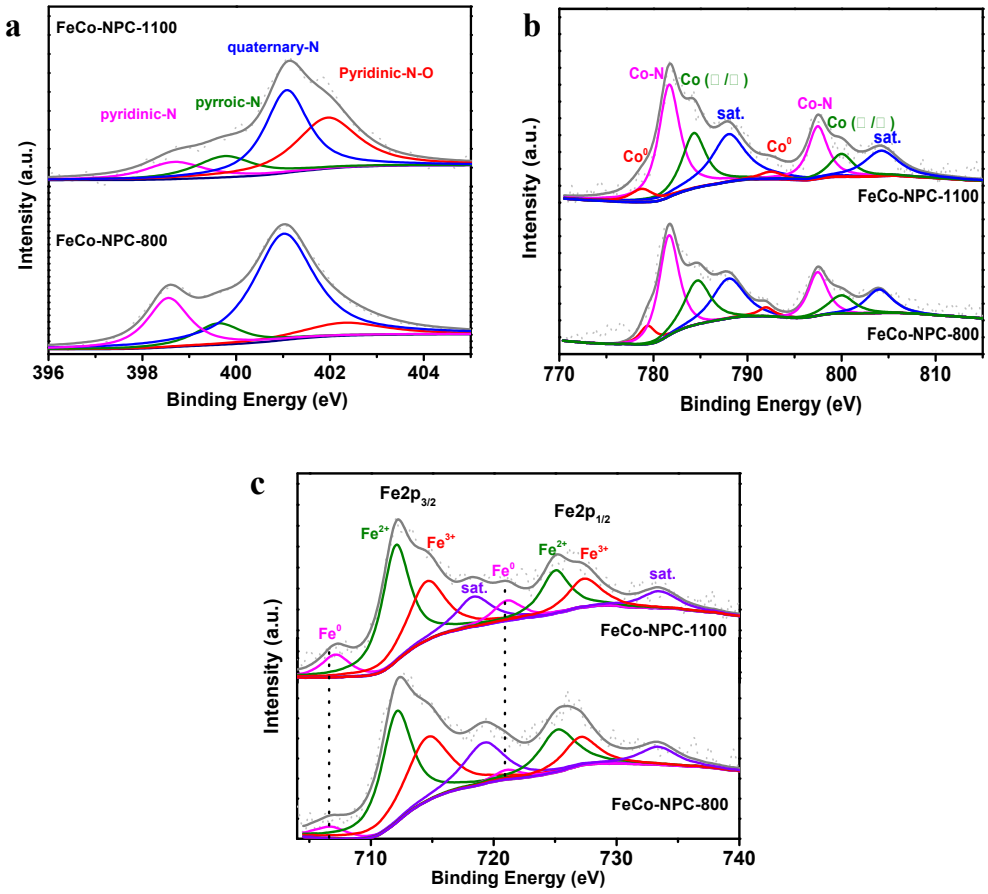

Fig. S5. XPS spectra of **a)** N1s, **b)** Co 2p, **c)** Fe2p for FeCo-NPC-1100 and FeCo-NPC-800.

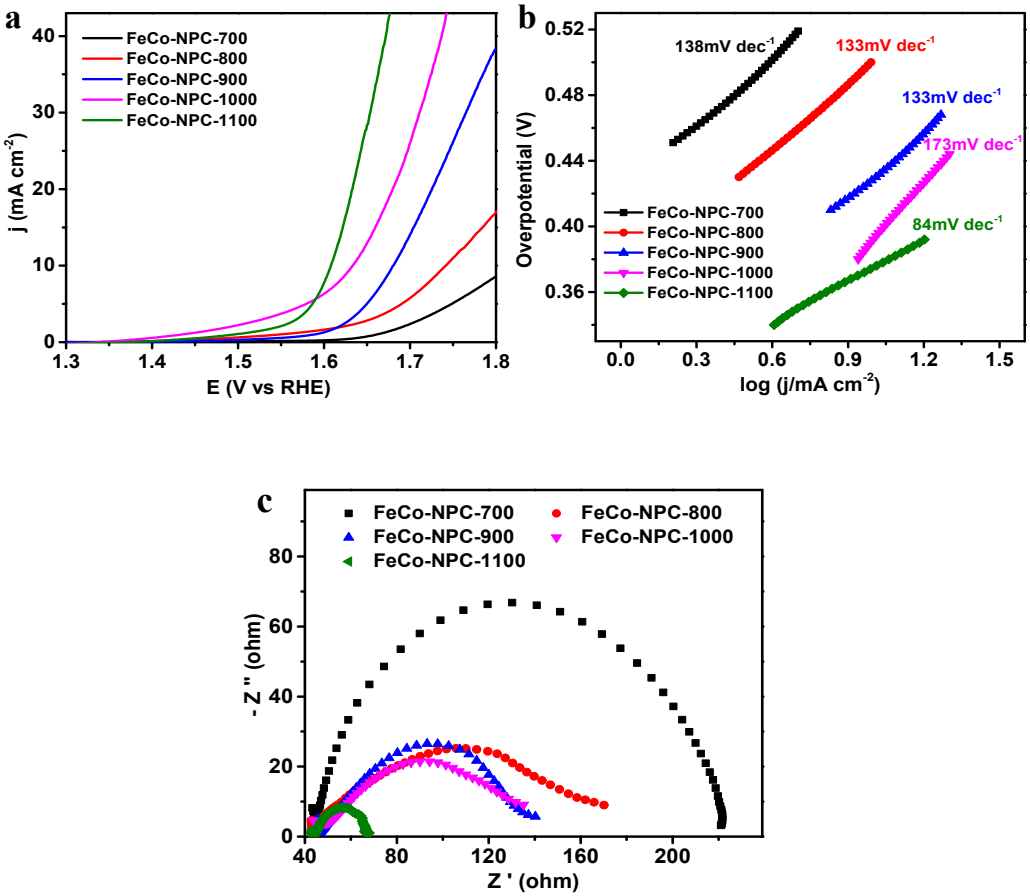

Fig. S6. a) OER polarization curves in O_2-saturated 0.1 M KOH (rotation rate: 1600 rpm); **b)** Tafel plots derived from (a); **c)** Nyquist plots at an overpotential of 370 mV

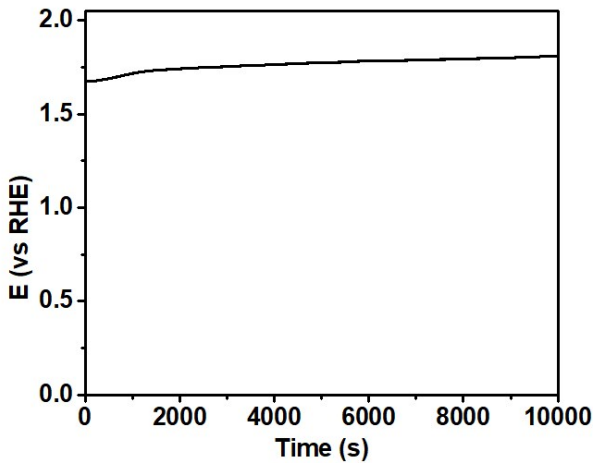

Fig. S7. Chronopotentiometric curve of FeCo-MPC-1100 in 0.1M KOH electrolyte at a current density of 10 mA cm^{-2}.

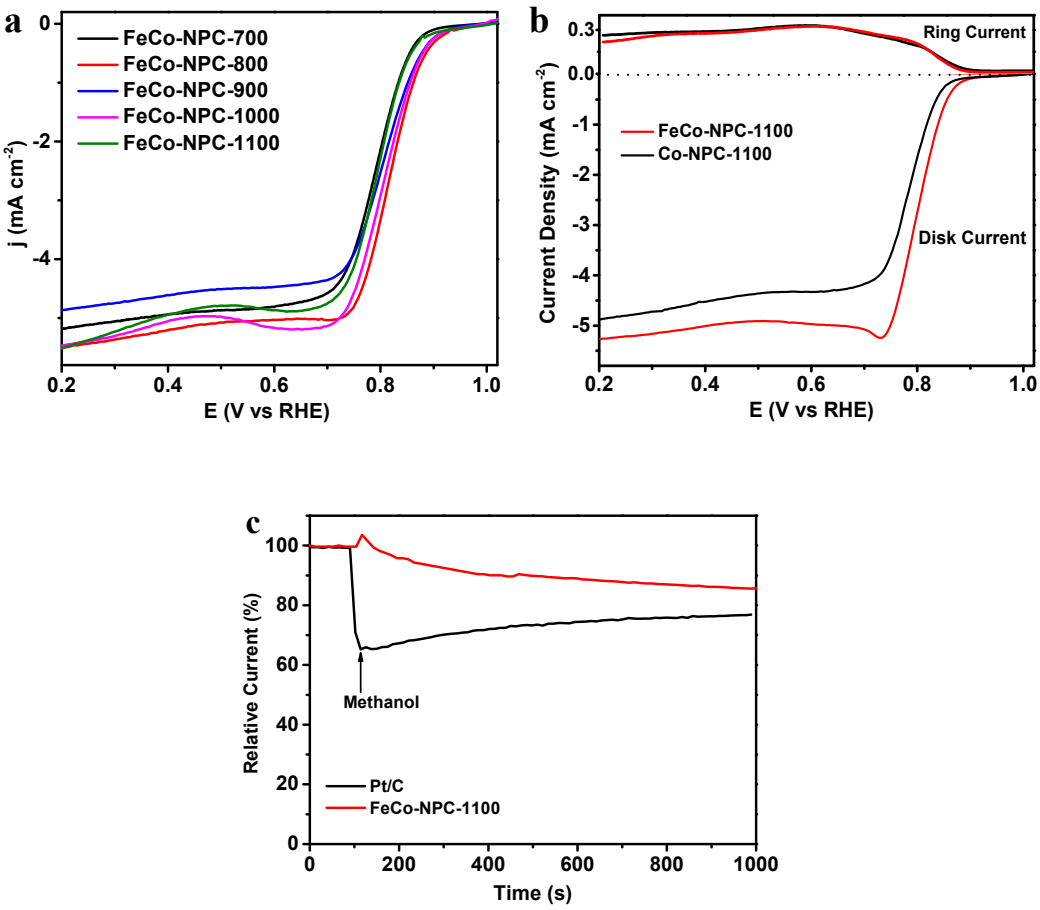

Fig. S8. a) ORR polarization curves in O_2-saturated 0.1 M KOH (rotation rate: 1600 rpm); **b)** Rotating ring-disk electrode (RRDE) voltammograms, **c)** comparison of chronoamperometric responses for FeCo-NPC-1100 and commercial Pt/C in O_2-saturated 0.1 M KOH electrolyte with 3 M methanol added at 100 s.

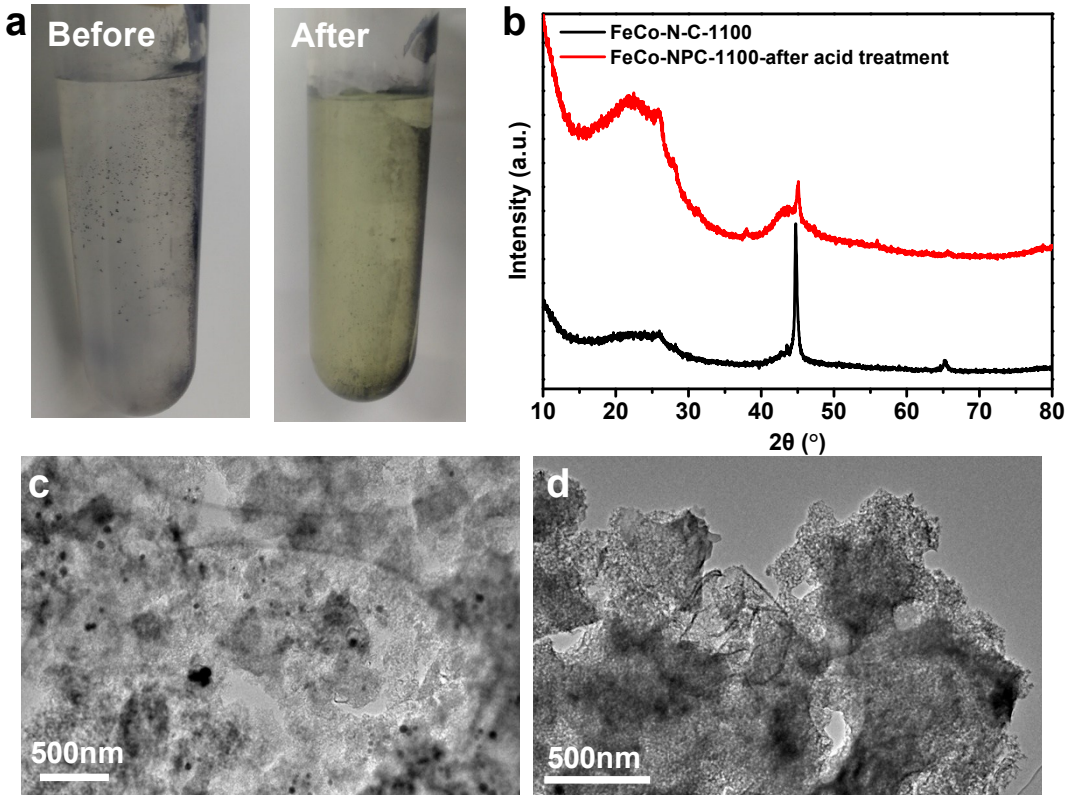

Fig. S9. a) Photograph and **b)** XRD patterns of FeCo-NPC-1100 before and after washed with 1M HCl; TEM image of FeCo-NPC-1100 **c)** before and **d)** after washed with 1 M HCl.

Table S1. The surface area and pore volume of resultant Co-NPC and FeCo-NPC catalysts.

Catalysts	S_{BET} ($m^2 g^{-1}$)	$V_{pore\ volume}$ ($cm^3 g^{-1}$)	$D_{pore\ diameter}$ (nm)
Co-NPC-1100	491	1.04	3.75
FeCo-NPC-1100	5601	1.01	6.49
FeCo-NPC-1000	1012	0.95	1.05
FeCo-NPC-800	718	0.71	6.46
FeCo-N-C-700	657	0.50	5.65

Table S2. A comparison in contents of Pyridinic N, Pyrrolic N, Quaternary-N, and Pyridinic-N-O species for resultant Co-NPC and FeCo-NPC catalysts calculated from their N 1s spectra.

Catalysts	Pyridinic N (at %)	Pyrrolic N (at %)	Quaternary-N (at %)	Pyridinic-N-O (at %)	Total N Content (at %)
Co-NPC-1100	6.7	6.7	49.6	37	1.00
FeCo-NPC-1100	11.3	13.7	39.9	35.1	1.11
FeCo-N-C-800	19.4	9.6	61.0	10	3.48

Table S3. A comparison in contents of Fe^0 and Fe^{n+} for FeCo-NPC-800 and FeCo-NPC-1100.

Catalysts	Fe^0 (at%)	Fe^{n+} (at%)	Total Fe Content (at%)
FeCo-NPC-1100	10.76	89.24	0.52
FeCo-N-C-800	6.7	93.3	0.62

Table S4. A comparison in contents of Co^0 and Co^{n+} for FeCo-NPC-800 and FeCo-NPC-1100.

Catalysts	Co^0 (at%)	Co^{n+} (at%)	Total Co Content (at%)
FeCo-NPC-1100	7.87	92.13	0.47
FeCo-N-C-800	6.02	93.98	0.66

Table S5. Comparison of the electrocatalyst performances of the prepared catalysts in 0.1 M KOH.

Catalysts	ORR onset potential (V vs.RHE)	ORR half-wave potential (V vs.RHE)	OER potential at 10mA/cm^2 (V vs.RHE)	ΔE (V)
Co-NPC-800	0.85	0.80	1.70	0.90
Co-NPC-1100	0.84	0.76	1.70	0.94
FeCo-NPC-700	0.87	0.78	1.82	1.04
FeCo-NPC-800	0.91	0.81	1.74	0.87
FeCo-NPC-900	0.90	0.80	1.68	0.88
FeCo-NPC-1000	0.9	0.80	1.62	0.82
FeCo-NPC-1100	0.88	0.79	1.60	0.81

Table S6. Summary of recently reported catalytic performances of FeCo based bifunctional oxygen electrodes in 0.1 M KOH, especially the ΔE, which indicates the potential difference between ORR half-wave-potential and OER potential at 10 mA/cm^2.

Catalysts	**ORR half-wave potential (V vs.RHE)**	**OER potential at 10mA/cm^2 (V vs.RHE)**	**ΔE (V)**	**References**
FeCo-NPC-1100	0.79	1.6	0.81	**This work**
CoFe/N-GCT	0.79	1.67	0.88	Angew. Chem. Int. Ed. 2018, 57, 16166.
N-GCNT/FeCo	0.92	1.73	0.81	Adv. Energy Mater. 2017, 7, 1602420.
meso/micro-FeCo-N_x-CN	0.89	1.67	0.78	Angew Chem Int Ed Engl 2018, 57, 1856
FeCo@CMS	0.85	1.67	0.82	Nanoscale, 2018, 10, 17021
FeCo/N-DNC	0.81	1.62	0.81	Nanoscale, 2018,10, 19937
FeCo/NPC	0.78	1.59	0.81	Adv. Sustainable Syst. 2017, 1, 1700020